Reservoir characterization in Leming Lake, Alberta

John J. Zhang and Laurence R. Bentley

ABSTRACT

This paper integrates well logs and lab measurements with seismic data to create a reservoir characterization model. The reservoir is located in Leming lake, Alberta, and ranges in depth from 410 m to 470 m approximately. It is characterized in well logs by low Gamma ray, low spontaneous potential and high electrical resistivity. The top and bottom picked in well logs demonstrate a relatively flat surface with regular geometry. The porosity obtained from core measurements and porosity logs clusters around 30%-40%. A small number of extremely low or zero values were found to come from strongly cemented limy sands or limestones. These tight rocks have a thickness around 2-3 m and appear to be irregularly distributed both vertically and horizontally. The reservoir framework is consequently viewed as a relatively homogeneous sand with irregularly spaced tight zones. Their occurrence was modeled with the universal Kriging. This conclusion is supported by seismic data acquired in a part of this area. Seismic reflections in the reservoir time window appear to come from tight rocks, which enabled us to find the details of these tight rocks and to establish a better reservoir characterization model.

INTRODUCTION

Heavy oil has been produced from the Clearwater formation in Leming Lake, Alberta, Canada. Recently Imperial Oil shot time-lapse three-D seismic surveys over a few production pads in an attempt to monitor fluid flow and reservoir conditions. Seismic interpretations for changes in saturation, pressure and temperature in reservoirs add another constraint on reservoir simulation in addition to production history matching. Reservoir management based on reservoir simulation optimized by both production performance and time-lapse seismic would enhance heavy oil recovery. In this paper the authors focus on integration of well logs and lab measurements with seismic data for a three-D reservoir characterization model, which will be modified in the future study to produce outputs consistent with production history and time-lapse seismic data.

RESERVOIR GEOMETRY

The study area is located in Leming Lake, Cold Lake, Alberta (Figure 1). The wells in red represent the area where reservoir characterization was conducted based on core measurements and well logs. A small area (Figure 1) was surveyed with three-D seismic repeatedly in 1997, 1998 and 1999 by Imperial Oil in an attempt to monitor steam injection and production for five horizontal wells. This part deals with the reservoir geometry obtained from well logs.

The Clearwater formation is bounded on bottom by the McMurray formation and on top by the Grand Rapids formation. It belongs to the upper Mannville group. A shale layer of a few meters on the top serves as a caprock to hold hydrocarbon. The oil saturated sands in the reservoir are identified in well logs by low Gamma ray, low SP potential, and high electrical resistivity. Figure 2 shows a typical set of well log curves at well 00/08-03-065-04W4/0. From shale to oil sands, SP, Gamma and resistivity logs

undergo a substantial change, while sonic, neutron porosity and density logs do not change significantly, which may make it difficult to seismically delineate the reservoir geometry. We picked the tops and the bottoms of the reservoir on all available well logs (Figure 3) in this area and fitted a second-order polynomial surface to the top and bottom boundaries. The error between the actual value and the one computed from trend analysis averages 4.7 meters. Figures 3 and 4 are a three-dimensional visualization of the reservoir geometry.

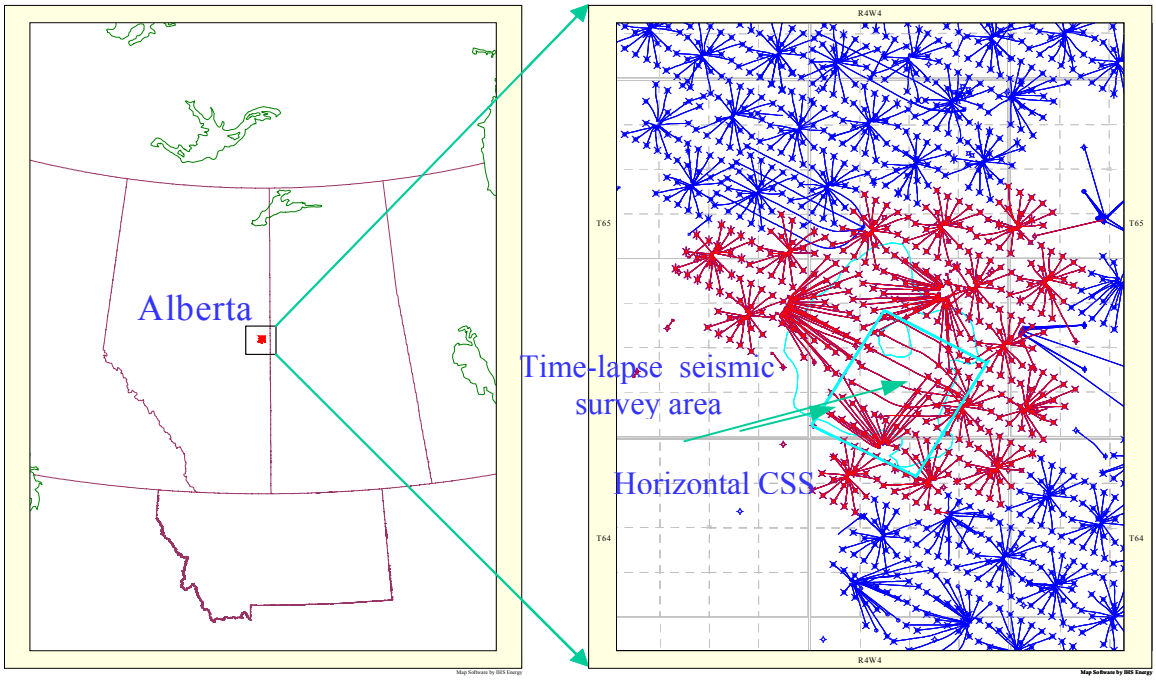

FIG. 1. Study area in Leming lake, Alberta.

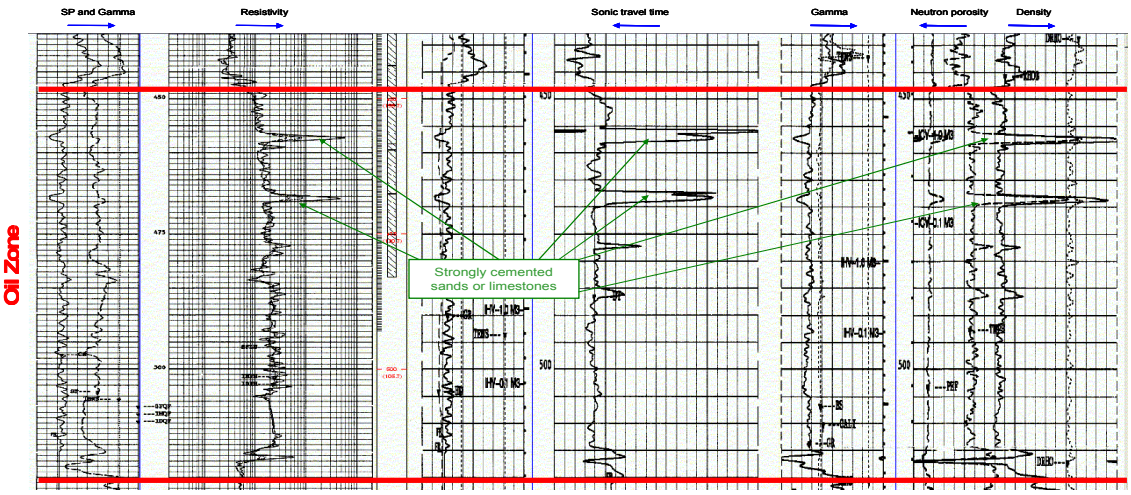

FIG. 2. Well logs for the Clearwater Formation at well 00/08-03-065-04W4/0.

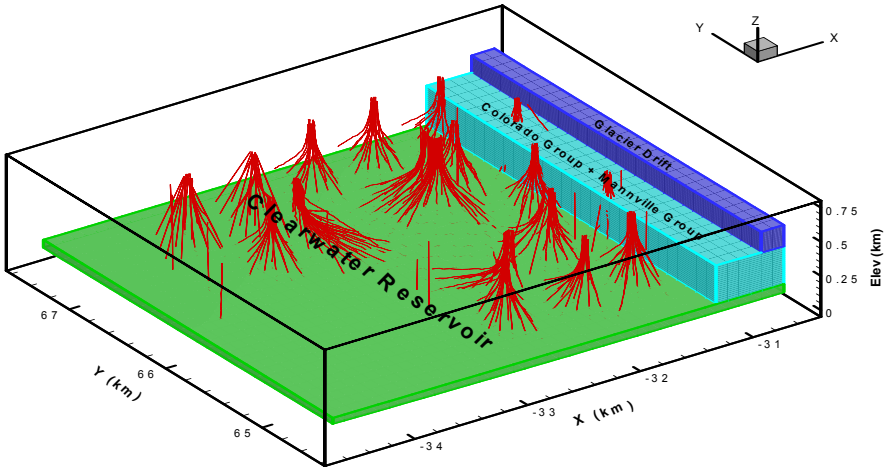

FIG. 3. Three-dimensional visualization of the reservoir geometry (x:eas, y:north, origin: 54^0,-110^0). The lines in red are wells.

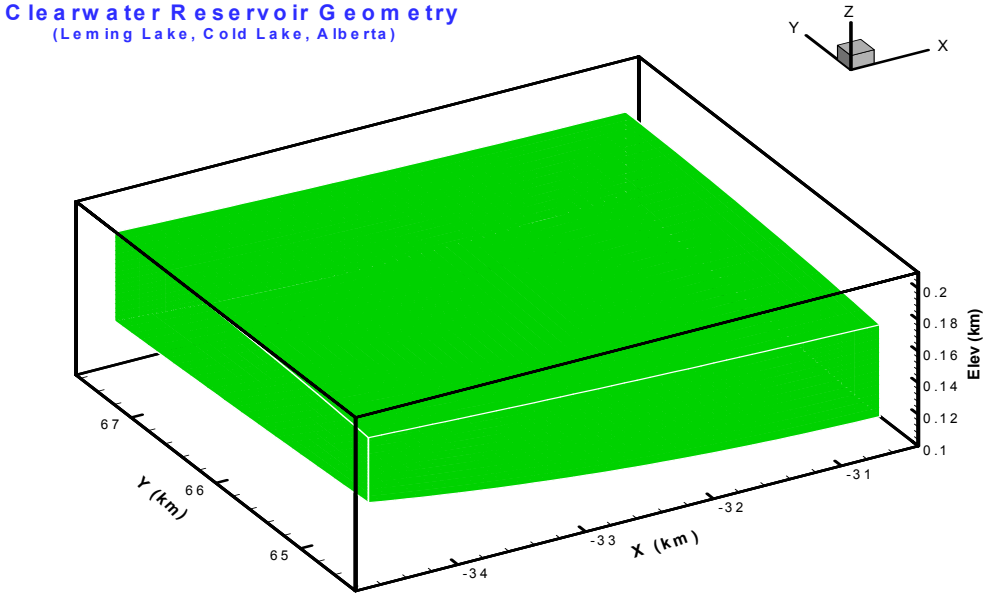

FIG. 4. Three-dimensional visualization of the reservoir geometry magnified (x:east, y:north, origin: 54^0,-110^0).

POROSITY POPULATION

The Clearwater reservoir is composed of unconsolidated sands with of limy cementations. Shale interbeds are less frequently encountered, as evidenced by flat Gamma logs throughout the zone (e.g., Figure 2). The histogram of Gamma ray logs for the reservoir (Figure 5) indicates overwhelming quantities of clean or slightly shaly sands.

Pure shales are rare and they probably do not constitute an important impermeable barrier to fluid flow within the reservoir.

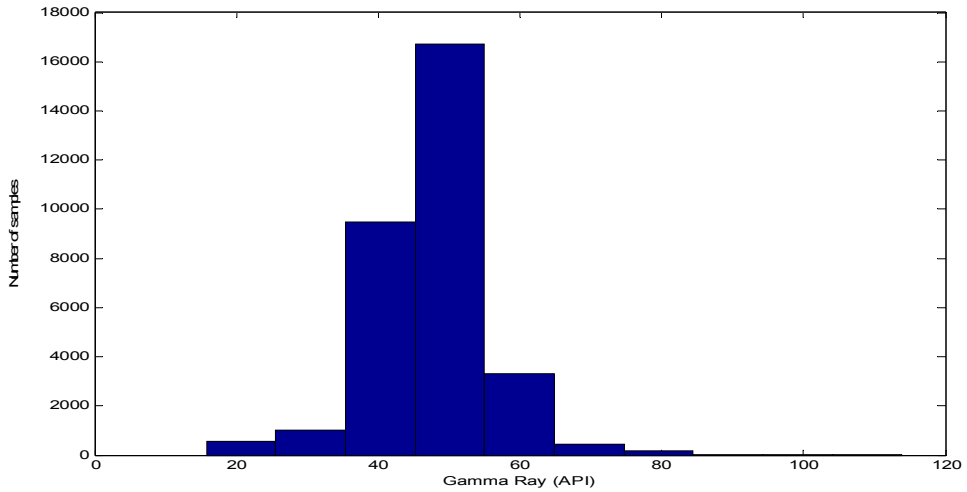

FIG. 5. Histogram of Gamma ray logs for the reservoir from forty-five wells

Cores were sampled continuously from top to bottom in fifteen wells. Porosity measurements of 2343 cores are mainly between 30% and 40% except a few with extremely low or zero values, as indicated in Figure 6. Lab reports (Figure 7) demonstrate that these few samples are chiefly from strongly cemented limy sands or limestone.

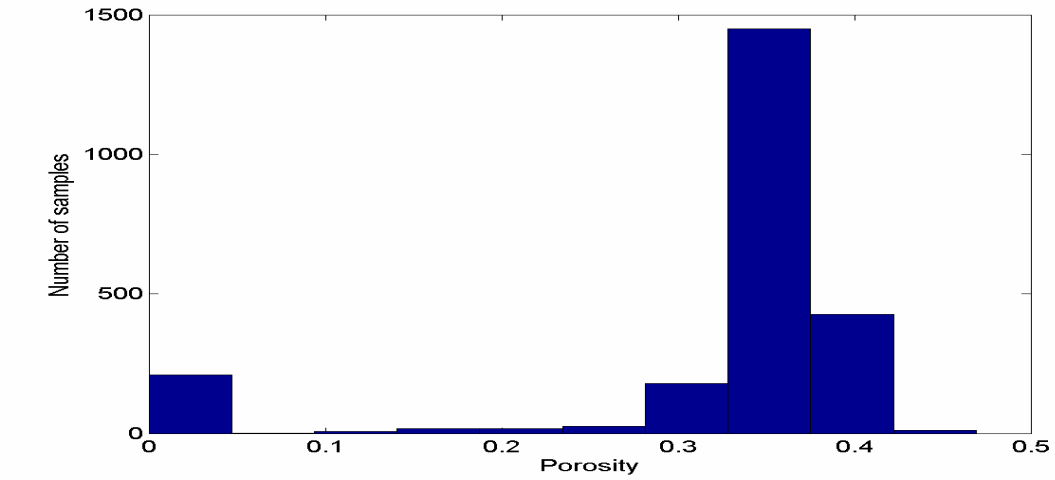

FIG. 6. Histogram of porosity measurements of cores.

H1392 fx Lithology

	A	B	C	D	E	F	G	H	I	J	K	L
1392	Location	Sample Ba	Thickness	SampleForms	Sample To	Porosity	KMax (mD	Lithology	RSat Oil R	RSat Wtr F	Bulk Dens	K90 (mD)
1393	AA/03-02-065-04W4/0	725.71	0.39	CLRWTSD	725.32	0	0	SS VF SHY LMY	0	0	0	0
1394	AA/03-02-065-04W4/0	726.12	0.41	CLRWTSD	725.71	0.357	0	SS VF F SSHY	0.776	0.224	0	0
1395	AA/03-02-065-04W4/0	726.67	0.55	CLRWTSD	726.12	0.361	0	SS VF F SSHY	0.674	0.326	0	0
1396	AA/03-02-065-04W4/0	726.82	0.15	CLRWTSD	726.67	0	0	SS VF SSHY LMY	0	0	0	0
1397	AA/03-02-065-04W4/0	727.35	0.53	CLRWTSD	726.82	0.362	0	SS VF F SSHY	0.776	0.224	0	0
1398	AA/03-02-065-04W4/0	727.89	0.54	CLRWTSD	727.35	0.339	0	SS VF F SSHY	0.726	0.274	0	0
1399	AA/03-02-065-04W4/0	728.38	0.49	CLRWTSD	727.89	0.353	0	SS VF F	0.718	0.282	0	0
1400	AA/03-02-065-04W4/0	728.88	0.5	CLRWTSD	728.38	0.35	0	SS VF F SSHY	0.71	0.29	0	0
1401	AA/03-02-065-04W4/0	729.38	0.5	CLRWTSD	728.88	0.346	0	SS VF F SSHY	0.741	0.259	0	0
1402	AA/03-02-065-04W4/0	729.89	0.51	CLRWTSD	729.38	0.346	0	SS VF F SSHY	0.712	0.288	0	0
1403	AA/03-02-065-04W4/0	730.39	0.5	CLRWTSD	729.89	0.349	0	SS VF F SSHY	0.726	0.274	0	0
1404	AA/03-02-065-04W4/0	730.87	0.48	CLRWTSD	730.39	0.361	0	SS VF F SSHY	0.684	0.316	0	0
1405	AA/03-02-065-04W4/0	731.39	0.52	CLRWTSD	730.87	0.351	0	SS VF F	0.684	0.316	0	0
1406	AA/03-02-065-04W4/0	731.88	0.49	CLRWTSD	731.39	0.348	0	SS VF F	0.691	0.309	0	0
1407	AA/03-02-065-04W4/0	732.48	0.6	CLRWTSD	731.88	0.335	0	SS VF F SSHY	0.651	0.349	0	0
1408	AA/03-02-065-04W4/0	732.85	0.37	CLRWTSD	732.48	0	0	SS VF SSHY LMY	0	0	0	0
1409	AA/03-02-065-04W4/0	733.37	0.37	CLRWTSD	733	0	0	SS VF SSHY LMY	0	0	0	0
1410	AA/03-02-065-04W4/0	733.79	0.42	CLRWTSD	733.37	0.333	0	SS VF F SSHY	0.462	0.538	0	0
1411	AA/03-02-065-04W4/0	733.98	0.19	CLRWTSD	733.79	0	0	SS VF SHY LMY	0	0	0	0
1412	AA/03-02-065-04W4/0	734.23	0.25	CLRWTSD	733.98	0.333	0	SS VF F SSHY	0.349	0.651	0	0
1413	AA/03-02-065-04W4/0	734.28	0.05	CLRWTSD	734.23	0	0	SS VF SHY LMY	0	0	0	0
1414	AA/03-02-065-04W4/0	734.38	0.1	CLRWTSD	734.28	0.333	0	AST SS VF F SSHY	0.349	0.651	0	0
1415	AA/03-02-065-04W4/0	734.88	0.5	CLRWTSD	734.38	0.351	0	SS VF F SSHY	0.642	0.358	0	0
1416	AA/03-02-065-04W4/0	735.38	0.5	CLRWTSD	734.88	0.361	0	SS VF F SSHY	0.736	0.264	0	0
1417	AA/03-02-065-04W4/0	735.89	0.51	CLRWTSD	735.38	0.337	0	SS VF F SSHY	0.564	0.436	0	0
1418	AA/03-02-065-04W4/0	736.39	0.5	CLRWTSD	735.89	0.353	0	SS VF F SSHY	0.766	0.234	0	0
1419	AA/03-02-065-04W4/0	736.89	0.5	CLRWTSD	736.39	0.353	0	SS VF F SSHY	0.75	0.25	0	0
1420	AA/03-02-065-04W4/0	737.4	0.51	CLRWTSD	736.89	0.347	0	SS VF F SLTST INCL	0.714	0.286	0	0
1421	AA/03-02-065-04W4/0	737.9	0.5	CLRWTSD	737.4	0.355	0	SS VF F SSHY	0.755	0.245	0	0
1422	AA/03-02-065-04W4/0	738.4	0.5	CLRWTSD	737.9	0.373	0	SS VF F SSHY SLTST INCL	0.745	0.255	0	0
1423	AA/03-02-065-04W4/0	738.9	0.5	CLRWTSD	738.4	0.376	0	SS VF F SLTST INCL	0.789	0.211	0	0

Sheet1 Sheet2 Sheet3

FIG. 7. Lab measurements of the Clearwater reservoir.

Porosity well logs can be used to estimate porosity. There are eleven wells in this area with neutron and density porosity logs in addition to conventional logs. In the reservoir zone, density logs correlate with porosity in a simple way and neutron porosity logs gauge pore spaces directly. Sonic logs can not readily be used to derive porosity. In fact the relationship of sonic logs and porosity does not exist in the porosity range of 30% to 40% in this area. As shown in Figure 8, the porosity histogram obtained from neutron porosity and density well logs of eleven wells is very similar in shape to the one in Figure 6. Most data fall within the range of 30% to 40%. The main difference is that the histogram contains no zero values. This is because neutron porosity and density well logs can detect the disconnected pores in limy sands or limestone while core measurements can not. The principle of deriving porosity from neutron porosity and density well logs is based on the following equations:

$$\phi_N = \phi\,\phi_{N\text{-}p} + V_{sh}\,\phi_{N\text{-}sh} + (1-\phi-V_{sh})\,\phi_{N\text{-}s}\,, \qquad (1)$$

and

$$\phi_D = \phi\,\phi_{D\text{-}p} + V_{sh}\,\phi_{D\text{-}sh} + (1-\phi-V_{sh})\,\phi_{D\text{-}s}\,, \qquad (2)$$

where ϕ_N, $\phi_{N\text{-}p}$, $\phi_{N\text{-}sh}$ and $\phi_{N\text{-}s}$ are neutron porosity log values for fluid-saturated sands, pore fluids, shale and solid grains respectively; ϕ_D, $\phi_{D\text{-}p}$, $\phi_{D\text{-}sh}$ and $\phi_{D\text{-}s}$ are density porosity

log values for fluid-saturated sands, pore fluids, shale and solid grains respectively; ϕ is the unknown porosity we want to solve; Vsh is the volume shale content. For clean wet sands or sandstones, $\phi_{N\text{-}p} = \phi_{D\text{-}p} = 1$, Vsh=0, $\phi_{N\text{-}s} = \phi_{D\text{-}s} = 0$. Equations (1) and (2) are

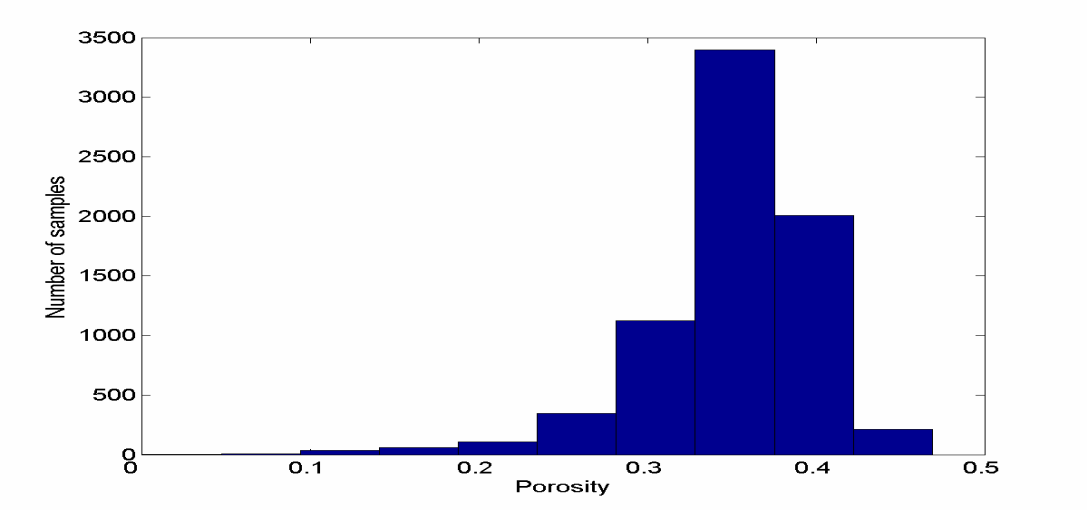

FIG. 8. Histogram of porosity obtained from porosity well logs.

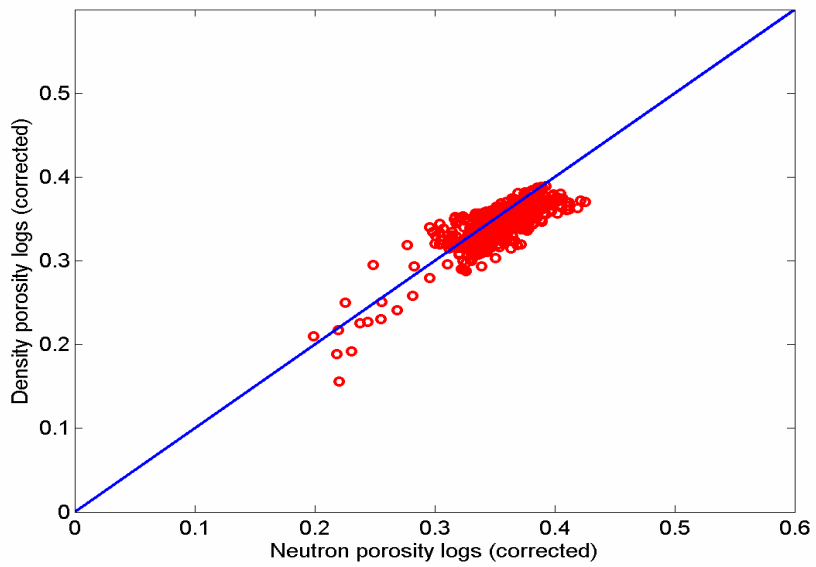

Figure 9 Cross plots of corrected neutron porosity versus corrected density porosity well logs

simplified as $\phi_N = \phi_D = \phi$. The cross plot of ϕ_N and ϕ_D is therefore a straight line y=x. In this area, however, sands are filled with both heavy oil and water and contain clay and limy cements. Corrections are necessary to be done to raw neutron porosity and density in order to obtain unknown porosity. Figure 9 is the cross plot of corrected neutron and density porosities from well 02/03-02-065-04W4/0. The correction was conducted to obtain ϕ according to equations (1) and (2). The parameters for correction are acquired in the following way. Neutron porosity and density porosity log values for a mixture of heavy oil and water (ϕ_{N-p} and ϕ_{D-p}) are nearly one. The volume shale content (Vsh) was computed from Vsh = (G - Gmin) / (Gmax - Gmin), where G is Gamma ray units, Gmin and Gmax are the minmum and maximum Gamma ray units, respectively. Generally, Gmin and Gmax take the values of pure sands and pure shale. ϕ_{N-sh} and ϕ_{D-sh} are ϕ_N and ϕ_D at G=Gmax. Neutron porosity log values for solid grains (ϕ_{N-s}) are zero, but density porosity log values for solid grains (ϕ_{D-s}) may be some value because grains include partly limy cements. If all the parameters are suitable, the corrected cross plot will cluster along the straight line y=x (Figure 9). If they deviate substantially, go back to well logs to select better parameters.

The predominance of porosity over the range of 30%-40% plus a few extremely low or zero values implies a relative homogeneous (clean or slightly shaly) sand with occasional limy sands or limestone streaks. If this reservoir character deduced from core measurements and well logs is representative of the whole area, reservoir characterization reduces to finding the distribution of these tight rocks, which, as significant barriers to fluid flow, are a key factor in reservoir production.

DISTRIBUTION OF TIGHT ROCKS

Within the oil zone in the Clearwater formation, strongly cemented limy sands or limestone are found in wells and are characterized in well logs by spikes of high resistivity, low sonic travel time, low neutron porosity and high density, as seen in Figure 2. We picked as strongly cemented sands or limestone the spikes of high resistivity in the oil zone for 250 wells, 27 of which were verified by sonic, neutron porosity and density logs. The number of these spikes at individual well locations is found to be randomly distributed, which may indicate the constant mean and variance of this variable as seen in Figure 10.

Based on the data from 250 well locations, a model variogram of the number of these spikes per well location was constructed using standard geostatistical procedures (Isaaks, 1989; Olivier, 2003) and is shown in Figure 11. The mathematical form for the model variogram is:

$$\gamma(h) = \gamma_0 + \gamma_1 [1-\exp(-3h/2)], \quad (3)$$

where $\gamma(h)$ is variogram, h is distance (km); γ_0 is 1.3; γ_1 is 0.7. From Equation (3), the number of strongly cemented limy sands or limestone for all grid locations in the reservoir x y plane was estimated using universal Kriging. Once the number of these tight zones at individual locations was assigned, their placements within the vertical section at

each grid location were randomly selected. The final result is seen in Figure 12, where porosity within the reservoir is dominated by the range between 30% and 40% with sparsely distributed strongly cemented limy sands or limestone.

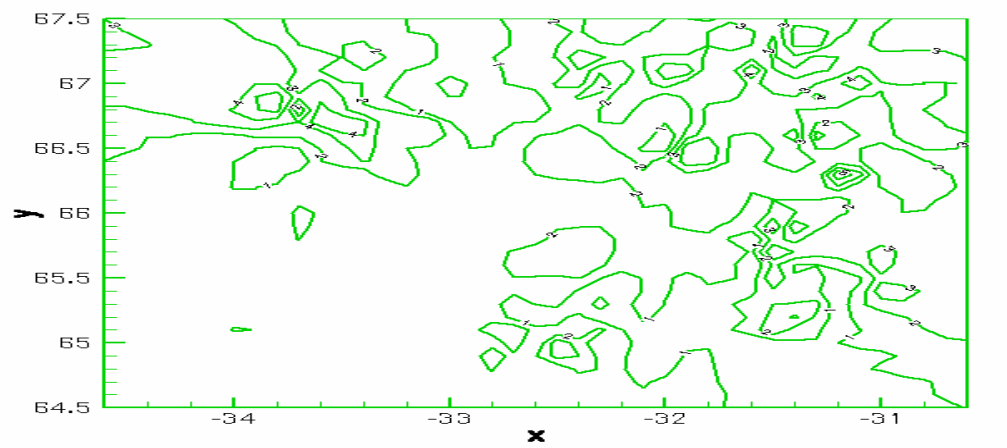

FIG. 10. Contour of the number of strongly cemented sands or limestones.

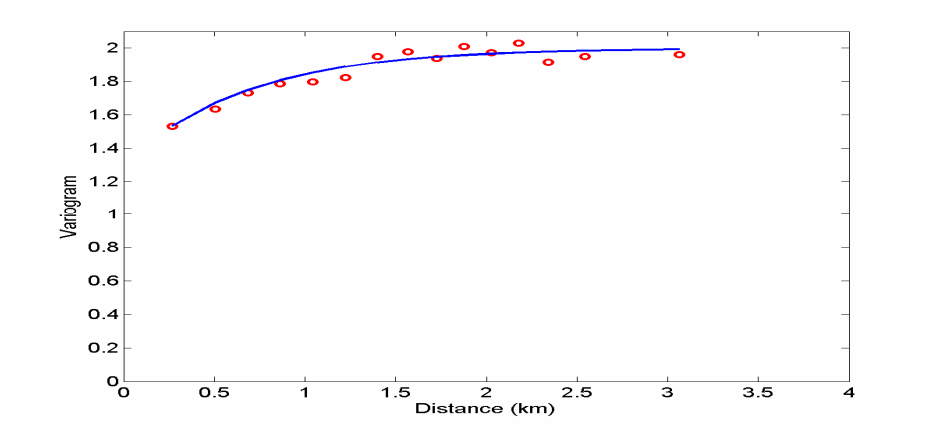

FIG. 11. Model of variogram with the number of limy sands or limestones as variable.

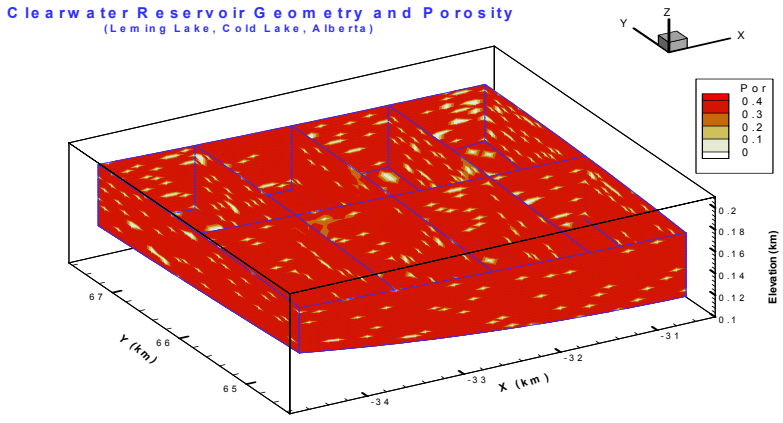

FiG. 12. Three-dimensional visualization of the reservoir geometry and porosity (x:east, y:north, origin: 54^0,-110^0). The model was created first by inverse-distance porosity interpolation from cores and well logs, and then by Kriging interpolation of tight rocks mentioned in the text.

SEISMIC ANALYSIS

Three-D seismic surveys were carried out in a small part of the area as shown in Figure 1, which provide another means to improve reservoir characterization. There are a few wells with sonic and density logs available to tie seismic sections (Figure 13).

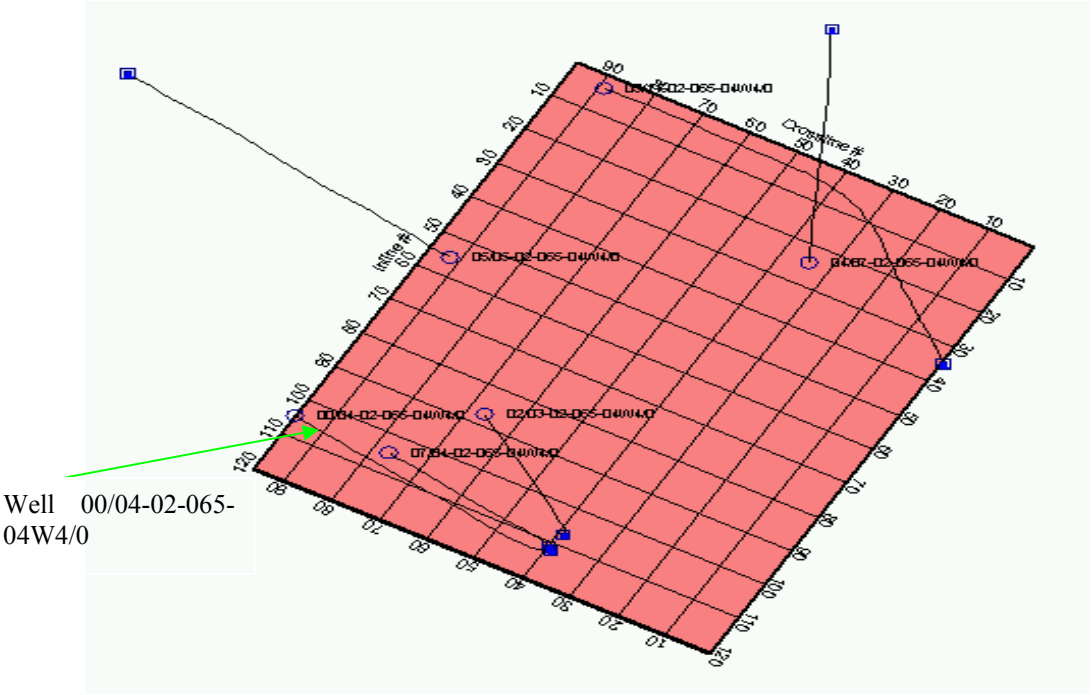

FIG. 13. 3-D seismic surveys in Leming lake, Cold lake, Alberta.

In Figure 14, well 00/04-02-065-04W4/0 is posted on the seismic section, which ties well with the synthetic seismic. The reservoir top on the seismic section was found to be located around 410 ms. The bottom is not penetrated by the well and can be estimated to be 410ms + 60m (thickness) / 2300m/s (velocity) *1000*2(two-way travel time)=460ms. For other wells the results do not differ substantially. Accordingly, the time window between 410ms – 460 ms is defined as the reservoir zone and any seismic attributes extracted from the zone can be interpreted for reservoir properties.

As discovered earlier, the reservoir is a relatively homogeneous sand with scattered limy sands or limestone. These tight rocks are not correlated horizontally from well observations and the universal Kriging method was used to predict them in areas without well control. However, horizontal well sample interval is over 100m, far lower than 3-D seismic sample interval of 10 m. The horizontal continuity of the tight zones unknown from well logs may be unraveled by seismic reflections. If seismic data can differentiate the tight rocks vertically, they can aid in defining the details of the tight rocks on smaller scale and solve the problem of horizontal continuity.

In Figure 15, synthetic seismogram appears to resolve every spikes of tight rocks. The wavelet used for synthetic seismic is Ricker wavelet with dominant frequency of 80Hz, which comes from the extracted wavelet from 3-D seismic data.

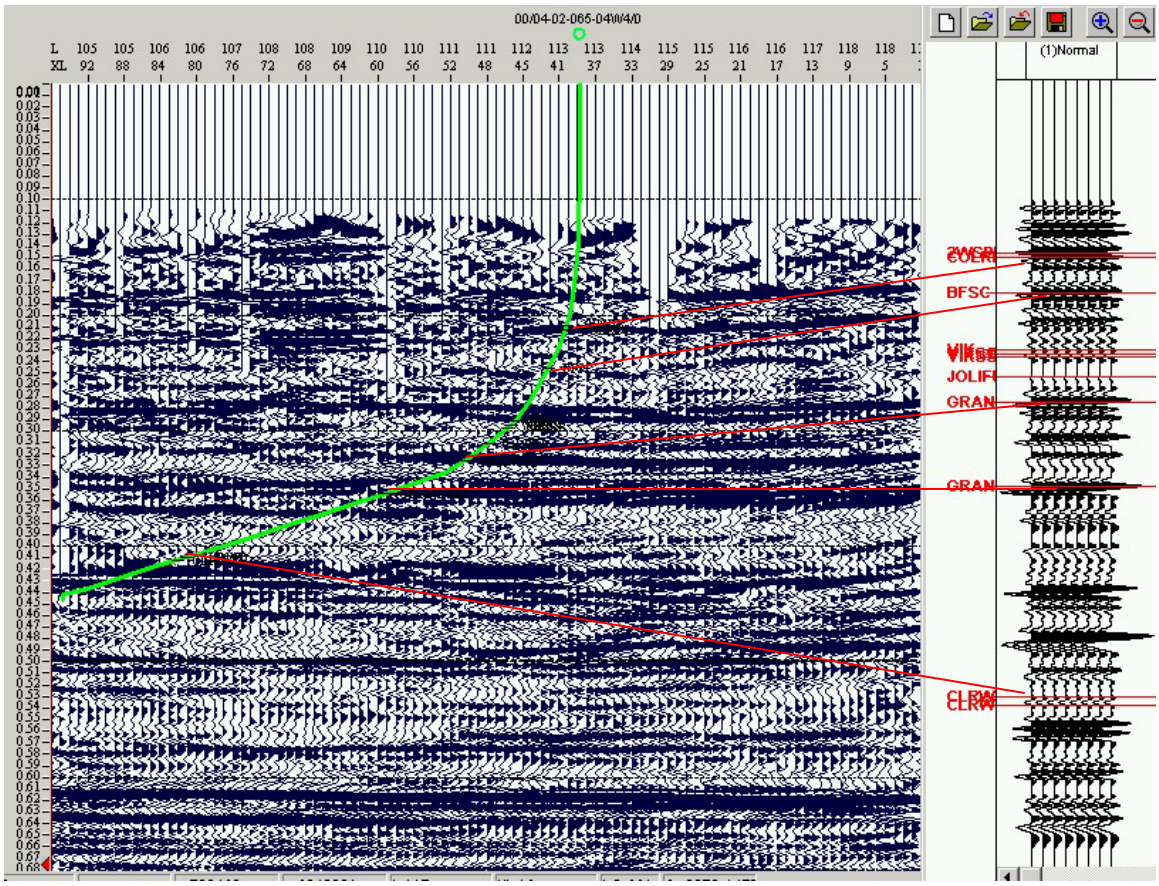

FIG. 14. Seismic section tied with synthetic seismogram for well 00/04-02-065-04W4/0.

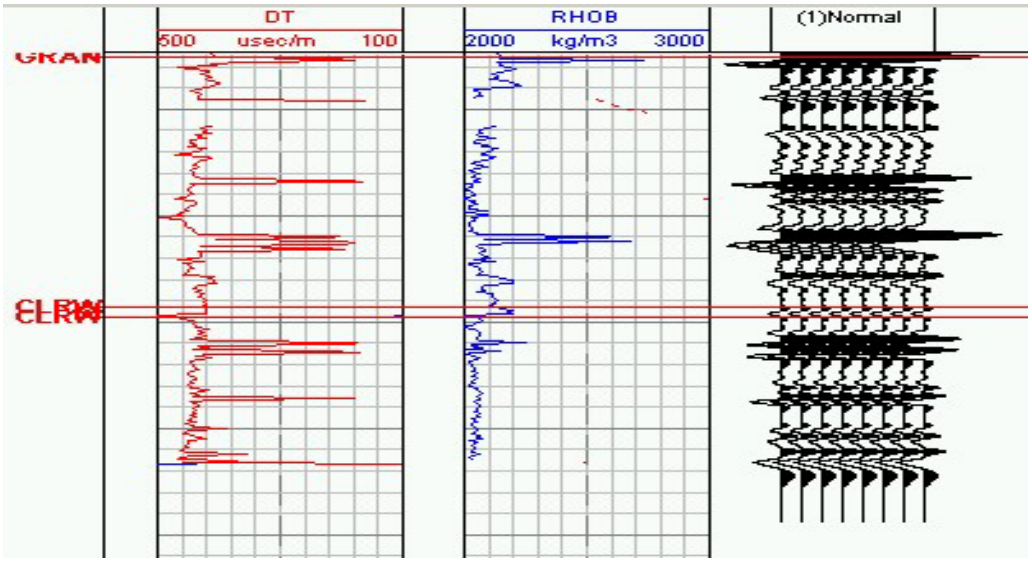

FIG. 15. Synthetic seismic traces, sonic and density logs for well 00/04-02-065-04W4/0.

To enhance seismic vertical resolution for better detection of tight rocks, the reservoir zone in the time window of 410-460 ms was deconvolved with the wavelet statistically extracted from 3-D seismic data. As shown in Figure 16 and 17, the strong reflection events become clarified, exhibiting local horizontal continuity. Sampled at an interval of 100 m, they do not seem spatially connected in most cases, which may support the

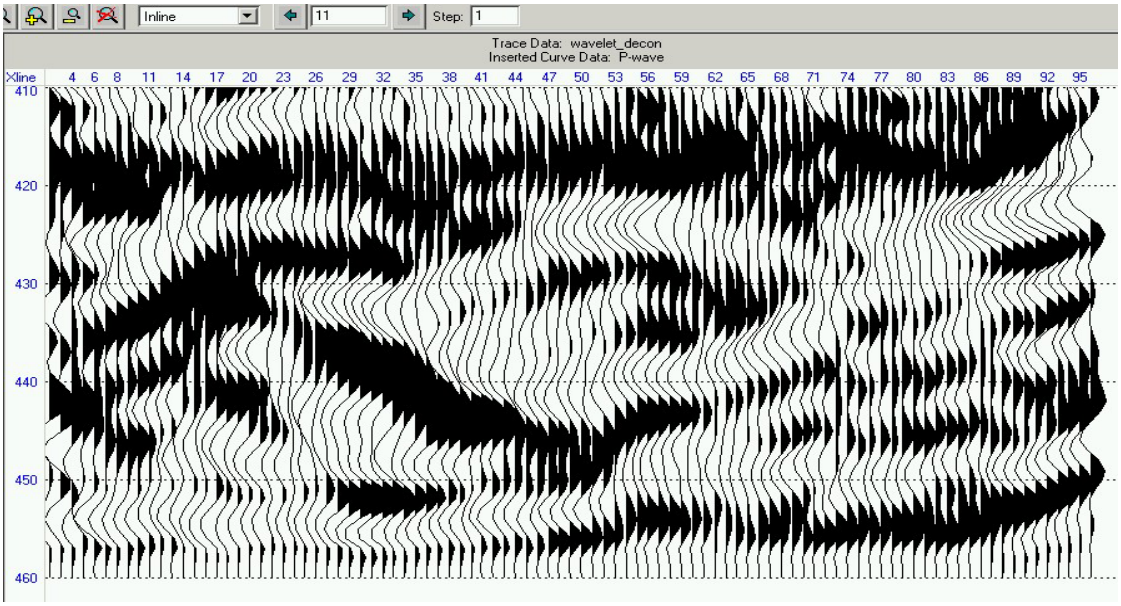

FIG. 16. Deconvolved seismic traces for the reservoir zone along inline 11.

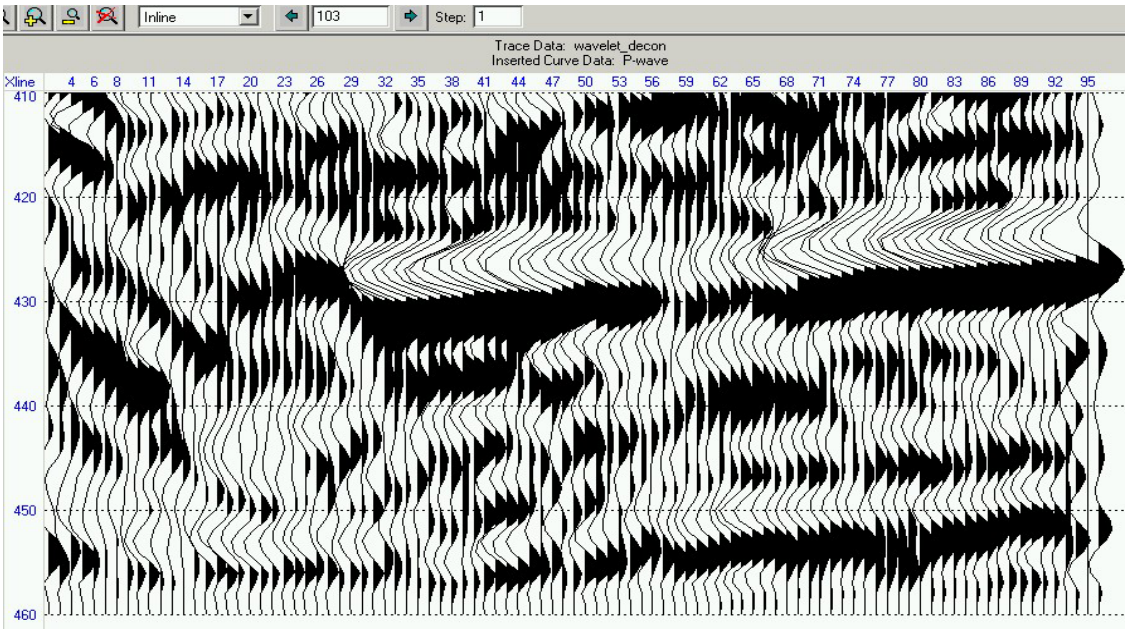

FIG. 17. Deconvolved seismic traces for the reservoir zone along inline 103.

assumption previously made from well logs. If these strong reflections truly come from tight rocks, it is feasible to reveal the detailed structures of these rocks using 3-D seismic data.

In the deconvolved time window of 410-460 ms, we picked the peaks for each trace of the 3-D seismic data volume, as seen in Figure 18, and assumed that they represented tight rocks. We further assumed the thickness of all tight rocks is two meters with zero porosity and permeability. As stated previously, the other part of the reservoir except these tight rocks is relatively homogeneous and porosity can be interpolated from known values of core measurements and well logs. We used inverse-distance interpolation to find the values in the reservoir. Then we put these tight rocks picked from the seismic data volume into the reservoir and finalized the population of porosity and permeability. Figures 19 is three-dimensional visualization of the distribution of porosity.

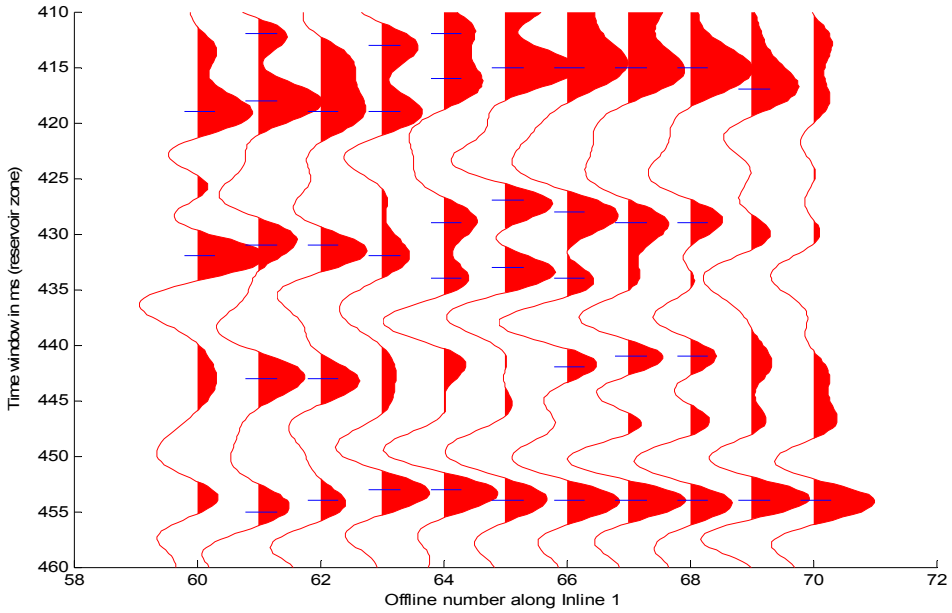

FIG. 18. Seismic traces and picks of amplitude peaks in the time window of 410-460 ms.

CONCLUSIONS

The Clearwater formation reservoir in Leming Lake, Alberta, Canada, is regular in geometry and has predominantly porosity between 30% and 40%. Strongly cemented limy sands or limestones are scattered within the reservoir and their occurrences can be stochastically modeled with the universal Kriging. Seismic reflections in the reservoir window appear to come from tight rocks, which enabled us to estimate the detailed structure of tight rocks and to establish a reservoir characterization model directly.

The distributions shown in Figure 19 were created using some arbitrary decisions and assumptions. In particular the assumption that every peak above a threshold represents a

tight zone is problematic. In addition, the threshold level was arbitrarily set. This procedure need to be validated and the model need to be compared to well logs in the area to see how well they correlate with observed tight zones.

ACKNOWLEDGEMENTS.

We would like to express our appreciation to the CREWES sponsors for their support of this research. We also gratefully acknowledge Imperial Oil for their permission to use their seismic data.

REFERENCES

Isaaks, E. H., 1989, Applied geostatistics: Oxford University Press.

Olivier, D., 2003, Geostatistics for seismic data integration in earth models: SEG and EAGE distinguished course

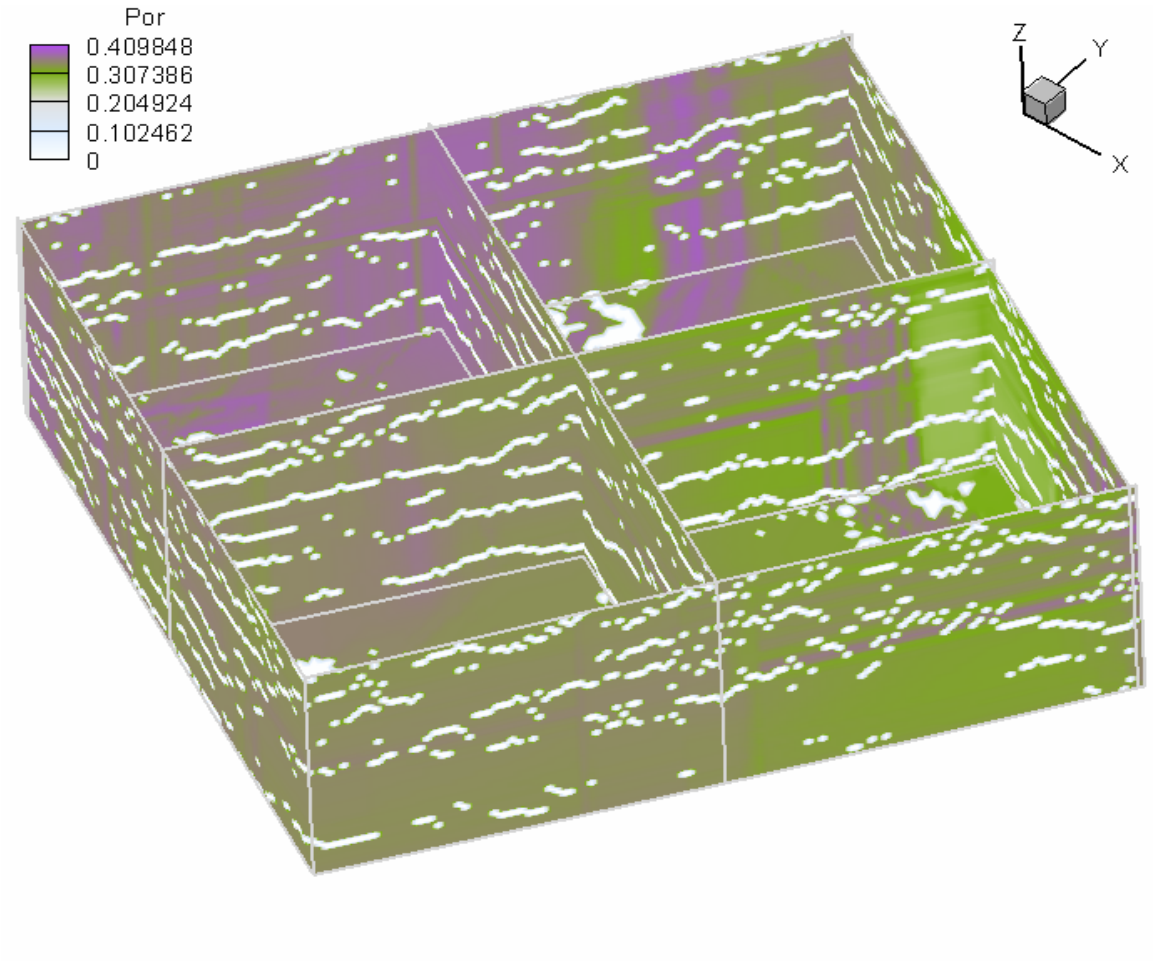

FIG. 19. Three-dimensional visualization of porosity in the area with seismic data (x:east, y:north, origin: 54^0,-110^0). The model was created first by inverse-distance porosity interpolation from cores and well logs, and then by putting tight rocks (zero porosity) picked from seismic traces into the reservoir.